Microchimica Acta
https://doi.org/10.1007/s00604-019-3261-8

ORIGINAL PAPER

Fluorometric determination of lipopolysaccharides via changes of the graphene oxide-enhanced fluorescence polarization caused by truncated aptamers

Hua Ye[1,2] · Nuo Duan[1] · Huajie Gu[1,3] · Haitao Wang[4] · Zhouping Wang[1,4,5,6]

Received: 9 November 2018 / Accepted: 16 January 2019

Abstract

A broad-spectrum ssDNA aptamer containing 80 nucleotides (LA80) and capable of binding to four different sources of lipopolysaccharides (LPSs) was truncated. Two strategies are used to produce truncated aptamers of different length. The results show that LA27, a 27-nt aptamer, retained broad-spectrum capability and has a higher affinity ($K_d = 46.2 \pm 9.5$ nM). A graphene oxide based fluorescence polarization assay (excitation/emission wavelengths: 485/520 nm) was worked out using FAM-labeled LA27. It can detect LPSs from *Salmonella entericaserotype typhimurium*, *Pseudomonas aeruginosa* 10 and *Escherichia coli* 055:B5 with enhanced performance (4.8 to 29-fold improvements) compared to LA80. The assay can be performed within 30 min, and the detection limits are 38.7, 88.0 and 154 ng·mL^{-1}, respectively.

Keywords Broad-spectrum aptamer · Binding region · Secondary structure · Biosensor

Introduction

Lipopolysaccharides (LPSs), also referred to as endotoxins, are primary components of the membranes of gram-negative bacteria and are extremely toxic to humans [1, 2]. LPS contamination is common in food and water products, therapeutic products, biological products [3]. A wide variety of biosensors have been applied in LPS detection, including protein-based biosensors [4], peptide-based biosensors [5], antibody-based biosensors [6]. Such biosensors have been greatly improved, in terms of their detection ability, over the years. However, aptamer-based biosensors [7–9] exhibit numerous advantages compared with other approaches. More precisely, they have high affinities and specificities with respect to their targets, good stabilities, and are easy to prepare and modify [10]. However, most aptamer-based LPS biosensor research has focused on materials used and sensor design and analytical procedures employed. There have been no attempts at downstream truncation or design of the aptamer itself, and all of the reported aptamers used for LPS detection are full length (70–100 nucleotides) [11–15].

It is widely accepted aptamers can fold into stable and specific three-dimensional structures and that they bind to their targets via intermolecular interactions, e.g. hydrogen bonding, van der Waals interactions, electrostatic forces, etc. However, not all of the bases or domains will take part in the aptamer-target binding process [16]. Indeed, some bases may interfere with the aptamers' ability to bind to their targets (affecting their specificity and binding affinity) because of the steric hindrance they cause [17]. For instance, Vu et al. found that truncating an initially long (86 nt) aptamer to a

Electronic supplementary material The online version of this article (https://doi.org/10.1007/s00604-019-3261-8) contains supplementary material, which is available to authorized users.

✉ Zhouping Wang
wangzp@jiangnan.edu.cn

[1] State Key Laboratory of Food Science and Technology, School of Food Science and Technology, Jiangnan University, Wuxi 214122, China

[2] College of Food Engineering, Anhui Science and Technology University, Fengyang 233100, China

[3] School of Chemical Biology and Materials Engineering, Suzhou University of Science and Technology, Suzhou 215009, China

[4] National Engineering Research Center of Seafood, School of Food Science and Technology, Dalian Polytechnic University, Dalian 116034, China

[5] International Joint Laboratory on Food Safety, Jiangnan University, Wuxi 214122, China

[6] Collaborative Innovation Center of Food safety and Quality Control of Jiangsu Province, Jiangnan University, Wuxi 214122, China

Published online: 15 February 2019

shorter one (36-nt) resulted in a 150-fold enhancement in binding affinity compared to the full-length aptamer [18].

In general, the full-length aptamers appearing in the SELEX library have three functional regions: a binding region, supporting region, and nonessential region [19]. The nonessential region corresponds to nucleotides that have neither a binding nor supporting role in relation to the molecular recognition process. Hence, identifying the effective binding region of aptamers is helpful to design and develop superior biosensors. In fact, this not only lowers the cost of aptamer synthesis but can also enhance the binding affinity [20–22]. Another important point to make is that it can help us understand the aptamer-target structure/activity relationship and thus broaden the application potential of the aptamer.

Fluorescence polarization (FP) is known to be a rapid, simple, and homogeneous assay technique that is commonly employed in analytical science [23]. FP values depend on the mass and local movement of fluorescently-labeled rotating molecules (for a given constant temperature and solution viscosity). However, the direct detection of the target signal in traditional FP assays is a somewhat inferior method as producing significant change in the FP signal is often very challenging. Thus, the detection limits are often very poor [24]. To overcome this problem, various different amplification strategies have been attempted. In particular, mass amplification strategies have been widely used to increase the sensitivity of the FP detection process in recent studies [25–28]. Of these methods, the use of graphene oxide (GO) has already proved to be an outstanding FP amplifier.

As is well known, the longer the aptamer, the more difficult it is to release it from the GO surface via target competition. This is because longer aptamers have stronger π stacking and electrostatic interaction with the GO surface, which also substantially decreases the FP detection sensitivity. Therefore, we surmise that truncated aptamers should improve the sensitivity of the GO-enhanced FP detection process. To investigate the feasibility of these proposition, a broad-spectrum ssDNA aptamer that can bind to four different sources of LPSs was chosen for truncating. The results showed that the truncated aptamer still retains a broad-spectrum capability and has a significantly improved sensitivity compared to its maternal aptamer in GO-based FP assay.

Materials and methods

Materials and instruments

All oligonucleotide sequences were synthesized by Integrated DNA Technologies (IDT) (Coralville, IA, USA, http://sg.idtdna.com/site) with HPLC purified. Graphene oxide (GO) power was purchased from Nanjing XFNANO materials Tech Inc. (Nanjing, China, https://www.xfnano.com/). Lipopolysaccharides from *Salmonella entericaserotype typhimurium* (LPS), *Salmonella enterica serotype enteritidis* (Se-LPS), *Escherichia coli* 055:B5 (Ecoli-LPS), *Pseudomonas aeruginosa* 10 (Pa-LPS) and L-α-phosphatidylcholine were purchased from Sigma-Aldrich (USA, http://www.sigmaaldrich.com). D-mannose was purchased from BBI Life Sciences Corporation (Cayman, http://www.bbi-lifesciences.com/), D-glucose was purchased from Sangon Biotechnology Co., Ltd. (Shanghai, China, http://www.sangon.com). Bovine serum albumin (BSA), Sucrose, Agar-agar power and Starch soluble were purchased from Sinopharm Chemical Reagent Co., Ltd. (Shanghai, China, http://www.sinoreagent.com). Sodium chloride injection comes from Tianjin jinyao group hubei tianyao pharmaceutical co. LTD (Tianjin, China, http://www.kingyork.biz/).

The characterization of GO was observed on JEM-2100HR Transmission electron microscopy (TEM) (JEOL Ltd., Tokyo, Japan, https://www.jeol.co.jp/) and Diemension ICON Atomic Force Microscope (AFM) (Bruker, Germany, https://www.bruker.com/). The FP value were measured on Synergy H1 multi-detection microplate reader (BioTek Instruments, Inc., USA, http://www.biotek.com). The black 96-well plates were purchase from Corning (USA, http://www.corning.com). The Isothermal Titration Calorimetric (ITC) experiment was performed on Microcal™ PEAQ ITC system (Malvern Instruments Limited, England, https://www.malvernpanalytical.com/en/).

Preparation of graphene oxide nanosheet

GO powder was dissolved in deionized water, and sonicated for 4 h in ultrasonic bath (KQ-800DE, total input power 800 W) with 40% power. The temperature of the bath was maintained 15–25 °C using homemade ice. After the pretreatment, 1 $mg{\cdot}mL^{-1}$ GO stocking solution was obtained and used for the preparation of working solutions.

Analysis of specificity

The specificity of the truncated aptamer was analyzed based on FP competition experiment. First, 75 μL of 30 $\mu g{\cdot}mL^{-1}$ GO was added to 75 μL of 10 nM aptamer and left to in dark for incubating 10 min at 37 °C, the fluorescence polarization values (mP) was recorded as mP_1.Then 50 μL of the target LPS (42 °C for 10 min before used) and interferent (Sucrose, D-mannose, D-glucose, EDTA, BSA, L-α-phosphatidylcholine, Agar-agar power and Starch soluble) was separately added to the previous mixture incubated for 20 min at 37 °C, the FP value was recorded as mP_2. The relative FP value ΔmP ($\Delta mP = mP_1 - mP_2$) was calculated and used to evaluate the specificity of the truncated aptamers. All experiments were performed in triplicate, and the average value was used.

Isothermal titration calorimetric (ITC)

The binding affinity between the aptamers and LPS was determined by ITC method at 25 °C. Each samples was dissolved in binding buffer (1 × BB, 50 mM Tris-HCl, 5 mM KCl, 100 mM NaCl, 1 mM $MgCl_2$, pH 7.4). Prior to measurement, each solution was thoroughly degassed by centrifuging for 15 min at 12000 rpm. The reaction cell was filled with the LPS solutions and the truncated aptamer was injected into the syringe. A typical titration consist of 19 injections with the first injection was set as 0.4 μL and all the subsequent injections was set as 2 μL each. The high feedback mode, 10 μCal·s^{-1} of reference power was chosen and the reaction cell was stirred continuously at 750 rpm with injection spacing time of 150 s, duration time of 4 s. The control titration of aptamer into BB at the same conditions was conducted to measure the heats of mixings and dilutions, which were subtracted from the titration data in the presence of LPS. The binding curve was analyzed using the one set of sites fitting model with MicroCal PEAQ-ITC Analysis Software to elucidate the Kd value.

Fluorescence polarization measurement and target detection

All fluorescence polarization measurements were carried out on Synergy H1 microplate reader using black, 96-well microplates. The excitation and emission wavelengths were set at 485 ± 20 nm and 520 ± 20 nm, respectively. G-factor correction was adjusted for all fluorescence polarization measurements to eliminate instrumental bias. For a typical target detection, LPS solutions was gradient diluted to different concentrations. 75 μL of 30 μg·mL^{-1} GO and 75 μL of 10 nM aptamer was incubating for 10 min in dark at 37 °C. Then 50 μL different concentrations of the target LPS (42 °C for 10 min before used) was separately added and incubated for 20 min at 37 °C. The ΔmP was calculated as mentioned above. All experiments were performed in triplicate, and the average value was used.

Results and discussion

Principles of aptamer truncation

Truncating the aptamer in a way that is rational or based on reasonable principles may lead to good results. Various strategies have been attempted in this sense, including sequentially deleting bases from the 3′ and/or 5′ end of the molecule [29], deleting the fixed primer region [30], analyzing the conserved sequences [31], intermolecular hybridization [18].

There is a view that the stem-loop structures which are formed by certain bases may constitute the region responsible for the binding of the aptamer to the target [32]. Rockey et al. have suggested that a rational and preferable approach to truncation is to be guided by the secondary structure of the aptamer [33]. Therefore, the broad-spectrum aptamer (LA80), which was previously selected according to capture-SELEX experiments carried out in our laboratory [34], was truncated mainly based on its predicted secondary structure.

LA80 contains 80 nucleotides with 20-nt subsequences at the 3′ and 5′ ends of the sequence. It is a broad-spectrum aptamer that can recognize four types of LPSs. The predicted secondary structure of LA80 suggests that it is an aptamer with obvious stem-loop structure (Fig. 1(a)). Two truncation strategies was used aiming to find the shortest sequence with strong specificity and high binding affinity. The first approach was to truncate the stem or loop, in turn, based on the secondary structure shown in Fig. 1(a). The convention adopted here is to name the truncated aptamer obtained in the form "LA+ base number". The second approach was to delete the fixed primer region (as suggested by Pan [30] which produced a 40-nt long random sequence and named LA40 (Fig. 1(b)). Overall, seven truncated aptamers sequences (LA60, LA54, LA48, LA36, LA27, LA22, and LA40) was obtained for further investigation.

Characterization of the truncated aptamers

The binding affinity and specificity of the truncated aptamer with respect to LPSs were analyzed. In order to improve the efficiency of the characterization process, the specificity was first investigated based on a competition test, as mentioned above.

As can be seen from the results in Fig. 2(a), truncation greatly affects the aptamers' specificity. However, they mostly retain the broad-spectrum characteristics that allow them to recognize three or four types of LPS, especially Pa-LPS and Ecoli-LPS. Also note that as the size of the aptamer decreases, the specificity gets better and better.

Among the possible interfering substances investigated, EDTA is known to commonly interfere in the current context. The shortest truncated aptamer LA22 can be seen to have a lowered specificity with respect to EDTA in these tests. It is also noteworthy that the random sequence LA40 is less affected and has better specificity compared to the longer aptamers LA60, LA54, and LA48. However, LA40 is also affected by EDTA.

Although LA36 has good specificity, the shorter LA27 is more advantageous in reducing the cost of synthesis. Therefore, based on the discussion above, LA27 was chosen for subsequent binding affinity analysis. An isothermal titration calorimetry experiment was carried out under optimal conditions (Fig. 2(b)) producing a K_d value for the binding between LA27 and LPS of 46.2 ± 9.5 nM. This is approximately half that of the original aptamer LA80 (K_d = 102 ±

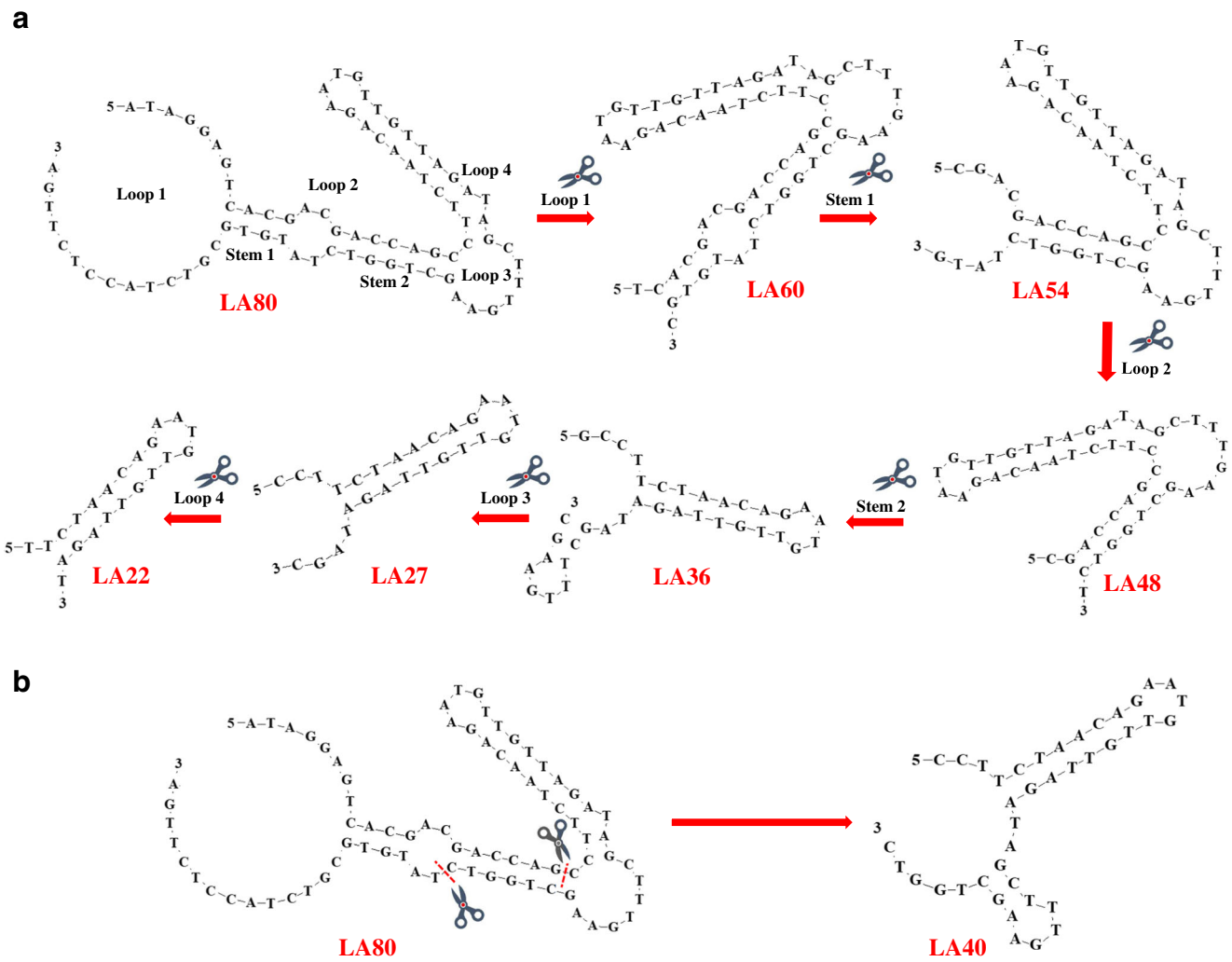

Fig. 1 The truncation strategies employed in this work based on (**a**) the secondary structure of LA80, and (**b**) the deletion of the fixed primer region

17 nM) [34]. Interestingly, as can be seen from Fig. 1, the LA27 sequence (obtained via truncation based on the secondary structure of LA80) corresponds to the first part of the LA40 sequence (at the 5′-end) which was obtained by deleting the fixed primer region. As mentioned before, LA40 is the central random region of the initial aptamer and other research

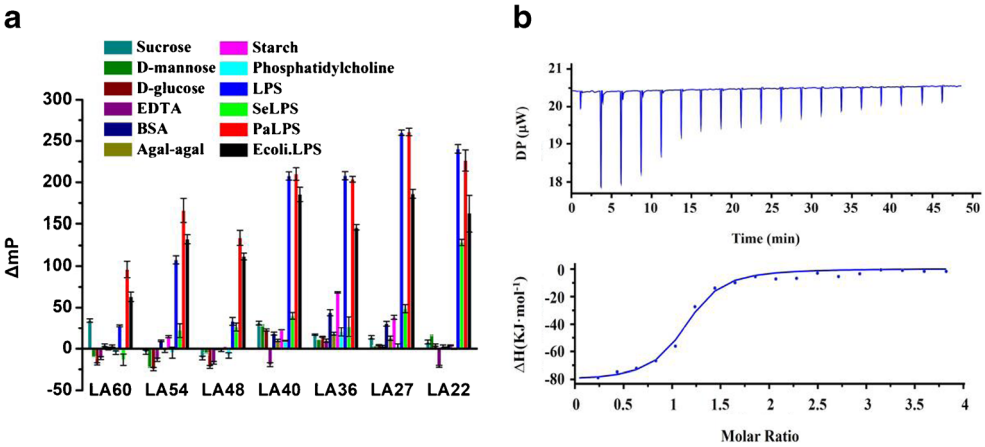

Fig. 2 **a** The specificity of the various truncated aptamers toward different targets including LPSs. **b** The binding affinity results obtained for LA27 against LPS

has indicated that the aptamer-target binding site may be located in the random region [30]. Therefore, LA27 was inferred as the core binding area between these aptamers and LPSs. All of these observations strongly suggest that truncation can enhance the binding affinity of the LPS aptamer and that LA27 is the optimal truncated aptamer to employ.

Optimization of the GO-enhanced FP assay conditions

A scheme illustrating the operation of the aptamer-based GO-enhanced FP assay process is shown in Fig. 3. The long aptamer was first truncated to a short one and then incubated with GO which is introduced as an FP signal amplifier to produce a large ΔmP value. When there is a target, the aptamer was captured by LPS and formed aptamer/target complex, resulting in a decrease in FP value compared to that without a target. In order to set up a reliable and rapid detection system, real-time kinetic tests were carried out to monitor the intensity and polarization of the fluorescence from the aptamer upon the addition of GO and LPS (Fig. 4).

First, it was checked whether a fluorescence recovery assay may work for detecting the LPSs directly. As shown in Fig. 4 (blue line), the LA27 initially produced a strong fluorescence intensity in the binding buffer because of the FAM-based dye. Then, after titration with 15 μg·mL^{-1} GO, the fluorescence intensity dropped sharply, from 4680 down to 90. This is due to the occurrence of fluorescence resonance energy transfer and electron transfer between the GO and FAM-labeled aptamer. However, when the target LPS was added, the fluorescence intensity only recovered to 230 (~5% of the original intensity). This indicates that a fluorescence recovery assay cannot be used to directly detect the LPS.

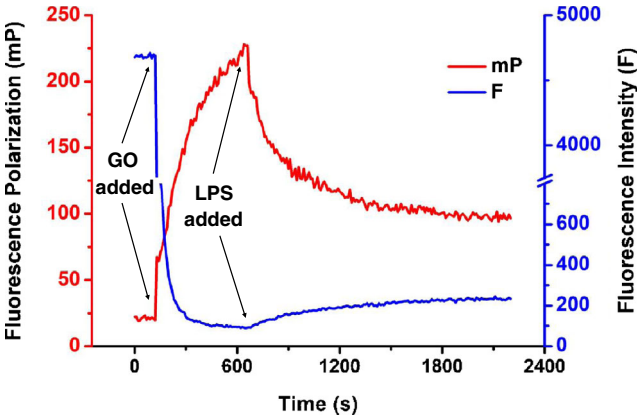

Fig. 4 Real-time kinetic test results for the FP (red line) and fluorescence intensity (blue line) measured from LA27 after the addition of GO and LPS

Then the changes in FP in the absence and presence of GO was measured. The results showed that the mP values do not change in an obvious way (by ~20) in the absence of GO (Fig. S2). This is because the molecular weight of the LPS-aptamer complex is not significantly increased compared to the

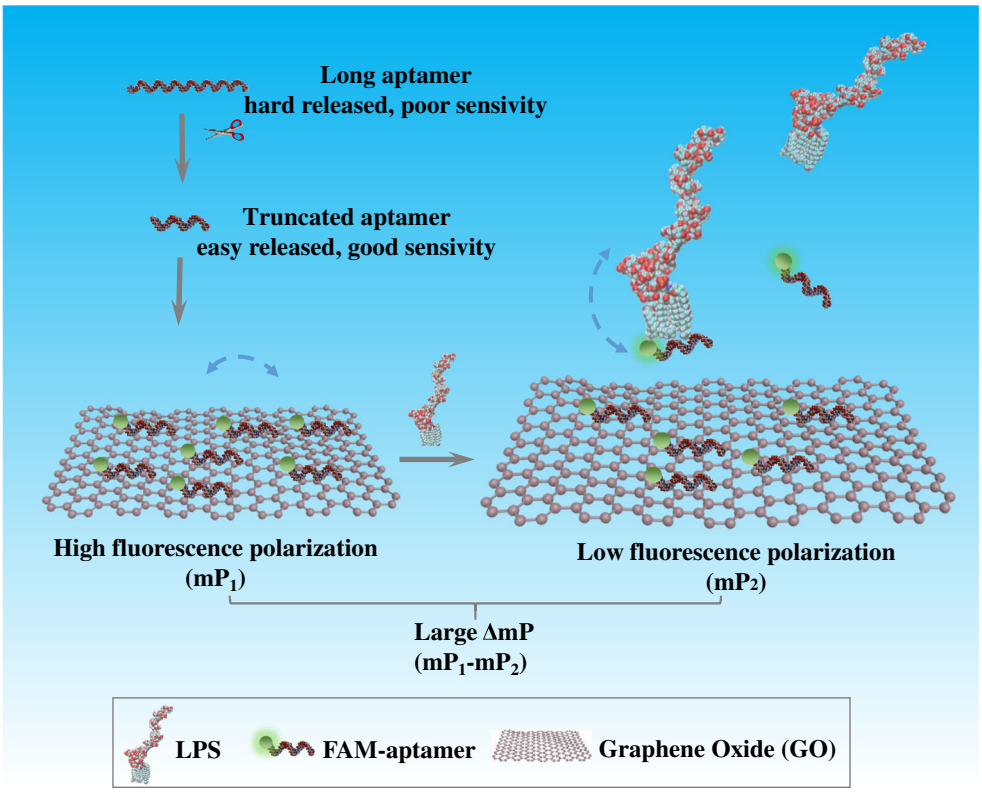

Fig. 3 Schematic presentation of the truncated aptamer based GO-enhanced FP assay process

aptamer. However, when GO is introduced as a signal enhancer, the mP values undergo a significant increase — from 20 up to 230 because of the large mass of the GO (Fig. 4, red line). This phenomena is in agreement with Liu's experimental results [26]. After LPS is added, the aptamer is released from the GO surface and captured by the LPS, forming a LPS-aptamer complex. This leads to a change in molecular weight and results in an obvious decrease in FP (from 230 to 95, a change of ~135), corresponding to an approximately 6.5-fold larger change than in the absence of GO. These results suggest that GO acts as a good FP signal amplifier and improves the sensitivity of the detection method.

The detection time was also optimized via real-time kinetic testing of the FP. After the addition of GO, the mP value increases significantly and reaches equilibrium after ~8 min (Fig. S3). This indicates that the sample assay can be carried out after the GO and aptamer have incubated for ~8 min. From Fig. 4, we can also see that after the target LPS has been titrated, the mP value decreases and reaches equilibrium after ~20 min. All these results strongly suggest that one sample can be detected within 30 min which guarantees that the detection process is rapid.

Detection of LPSs using LA27 and LA80

As the truncated aptamer LA27 retains a good ability to recognize LPS, Pa-LPS, and Ecoli-LPS, these three types of LPS were used to compare the detection limits available using LA27 and LA80. Therefore, to determine the sensitivity of LA27, dose-dependent experiments was carried out using the three types of LPS and both LA27 and LA80. The experiments were based on GO-amplified FP assays in sodium chloride injection samples.

The measured differences ΔmP (= $mP_1 - mP_2$) are plotted for the different types of LPS as a function of concentration in Fig. 5. As can be seen, in each experiment, the ΔmP values increase as the LPS concentration increases and there are good linear correlations over a certain range. However, the performance of the assays made using the truncated aptamer LA27 (in terms of linearity) is superior to those made using the original aptamer LA80 for each of the different LPSs. It also has a better responses at lower concentrations (See Table S2).In addition, the detection limits (3σ/S) obtained using LA27 with respect to LPS, Pa-LPS, and Ecoli-LPS were enhanced down to 38.7, 88.0, and 154 ng·mL^{-1} compared to the full-length aptamer LA80 (0.185, 2.56 and 2.82 μg·mL^{-1}). These figures approximately correspond to 4.8-, 29-, and 18-fold improvements, respectively. The results indicate that the truncated aptamer LA27 performs significantly better than the untruncated aptamer LA80. There are two main reasons for this. The first is that the shorter aptamer has weaker π stacking interactions with the GO compared to longer ssDNA sequences [35]. In other words, LA27 is more readily released from the GO surface and captured by the target, even when the concentration of the LPS is low. The other reason is that LA27 has some nonessential nucleotides removed which helps reduce steric hindrance. Of course, it still retains the core binding region leading to improved binding affinity and specificity

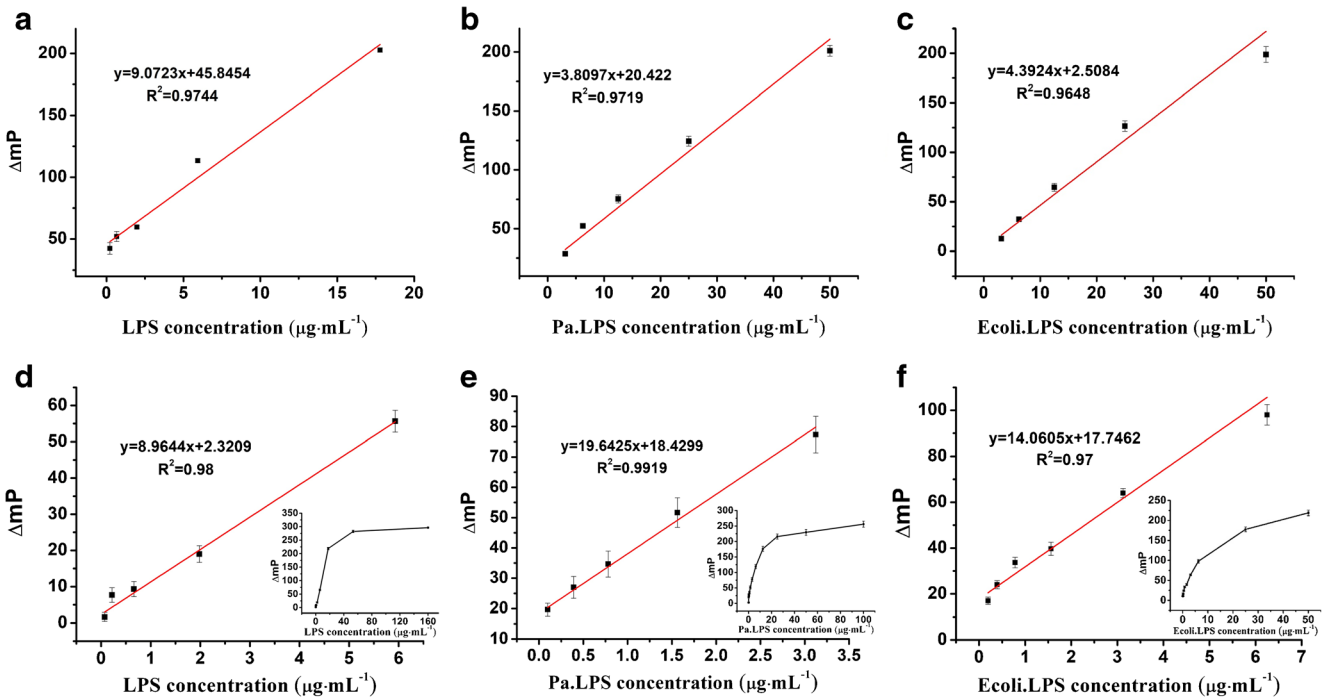

Fig. 5 Plots to determine the detection limits of the GO-enhanced FP assay technique using (**a**)-(**c**) LA80, and (**d**)-(**f**) LA27. In each set, the graphs correspond to LPS, Pa-LPS, and Ecoli-LPS, respectively

Table 1 The recovery of LPS in sodium chloride injection samples determined using the truncated-aptamer GO-enhanced FP assay technique

LPS source	Spiked concentration (ng mL^{-1})	Detected concentration, *mean* ± *SD* (ng mL^{-1})	Recovery rate (%)
LPS	10.0	10.31 ± 1.1	103.1
	50.0	48.6 ± 2.9	97.2
	100	92.0 ± 9.1	92.0
Pa-LPS	10.0	9.51 ± 1.1	95.1
	100	93.3 ± 7.1	93.3
	500	523 ± 15	104.6
Ecoli-LPS	50.0	56.2 ± 7.1	112.4
	100	93.2 ± 8.6	93.2
	500	477 ± 23	95.4

of the aptamer with respect to LPS. However, the molecular mechanism of the interaction between LA27 and LPS need to further study.

Table S3 gives an overview on recently reported methods for the determination of LPSs. As can be seen, aptamer-based fluorescence assay is a litter better than peptide-based method. Although electrochemical assay achieved an excellent sensitivity, its fabrication and preparation process is more complicated and tedious. Furthermore, LA27 is a shorter and broad-spectrum aptamer.

The truncated aptamer was also used as bioprobe to perform GO-enhanced FP assays on sodium chloride injection samples spiked with different concentrations of LPS, Pa-LPS, and Ecoli-LPS and thus carried out standard addition tests (Table 1). The results show that good recovery rates can be achieved after spiking (92–103.1%, 93.3–104.6%, and 93.2–112.4% for LPS, Pa-LPS, and Ecoli-LPS, respectively). This suggests that the truncated aptamer-based assay technique has good potential applicability to the detection of LPSs in real samples.

Conclusions

In this work, a broad-spectrum LPS aptamer was successfully truncated from 80 nucleotides long to 27 nucleotides. It was found that by eliminating the nonessential regions, LA27 has doubled the binding affinity and still has retained broad-spectrum superiority to the target. The LA27 and its maternal aptamer was subsequently used to conduct GO-based FP assays to rapidly detect LPSs. The results showed that the shorter aptamer LA27 has tremendously improved sensitivity with the range of 4.8- to 29-fold compared to its maternal aptamer LA80. In addition, the assay can be accomplished within 30 min. The results indicated that LA27 maybe the effective binding region of the aptamer and proved that truncated aptamers can improve the binding affinity and enhanced the sensitivity of GO-based FP assays. Furthermore, the truncated aptamer can be extended to other detection platforms construction and development for ultrasensitive detection of LPSs.

Acknowledgments This work was financially supported by the S&T Support Program of Jiangsu Province [BE2017623], Jiangsu Agriculture Science and Technology Innovation Fund [CX(18)2025], the National Natural Science Fund of China [31871881], the Fundamental Research Funds for Central Universities [JUSRP51714B], the Technology R&D Program of Suzhou [SNG2018044], the Distinguished Professor Program of Jiangsu Province and Jiangnan University Postgraduate Overseas Research Project.

Compliance with ethical standards The author(s) declare that they have no competing interests.

References

1. Gutsmann T, Schromm AB, Brandenburg K (2007) The physicochemistry of endotoxins in relation to bioactivity. Int J Med Microbiol 297(5):341–352. https://doi.org/10.1016/j.ijmm.2007.03.004
2. Bose S, Song MY, Nam JK, Lee MJ, Kim H (2012) In vitro and in vivo protective effects of fermented preparations of dietary herbs against lipopolysaccharide insult. Food Chem 134(2):758–765. https://doi.org/10.1016/j.foodchem.2012.02.175
3. Gorbet MB, Sefton MV (2005) Endotoxin: the uninvited guest. Biomaterials 26(34):6811–6817. https://doi.org/10.1016/j.biomaterials.2005.04.063
4. Ebrahim S, Reda M, Hussien A, Zayed D (2015) CdTe quantum dots as a novel biosensor for Serratia marcescens and Lipopolysaccharide. Spectrochim Acta A Mol Biomol Spectrosc 150:212–219. https://doi.org/10.1016/j.saa.2015.05.042
5. Lim SK, Chen P, Lee FL, Moochhala S, Liedberg B (2015) Peptide-assembled graphene oxide as a fluorescent turn-on sensor for lipopolysaccharide (endotoxin) detection. Anal Chem 87(18):9408–9412. https://doi.org/10.1021/acs.analchem.5b02270
6. Schenk F, Weber P, Vogler J, Hecht L, Dietzel A, Gauglitz G (2018) Development of a paper-based lateral flow immunoassay for simultaneous detection of lipopolysaccharides of salmonella serovars. Anal Bioanal Chem 410(3):863–868. https://doi.org/10.1007/s00216-017-0643-9

7. Xu W, Tian J, Shao X, Zhu L, Huang K, Luo Y (2016) A rapid and visual aptasensor for lipopolysaccharides detection based on the bulb-like triplex turn-on switch coupled with HCR-HRP nanostructures. Biosens Bioelectron 89:795–801. https://doi.org/10.1016/j.bios.2016.10.012
8. Posha B, Nambiar SR, Sandhyarani N (2018) Gold atomic cluster mediated electrochemical aptasensor for the detection of lipopolysaccharide. Biosens Bioelectron 101:199–205. https://doi.org/10.1016/j.bios.2017.10.030
9. Zhao M, Chen AY, Huang D, Chai YQ, Zhuo Y, Yuan R (2017) MoS2 quantum dots as new Electrochemiluminescence emitters for ultrasensitive bioanalysis of lipopolysaccharide. Anal Chem 89(16):8335–8342. https://doi.org/10.1021/acs.analchem.7b01558
10. Wu J, Zhu Y, Xue F, Mei Z, Yao L, Wang X, Zheng L, Liu J, Liu G, Peng C, Chen W (2014) Recent trends in SELEX technique and its application to food safety monitoring. Microchim Acta 181(5–6):479–491. https://doi.org/10.1007/s00604-013-1156-7
11. Kim S-E, Kim D-K, Han A-R, Choe W-S (2012) Screening of lipopolysaccharide binding DNA aptamer and its application to fabricating electrochemical aptasensor. New Biotechnol 29:S169. https://doi.org/10.1016/j.nbt.2012.08.470
12. Su W, Cho M, Nam J-D, Choe W-S, Lee Y (2013) Aptamer-assisted gold nanoparticles/PEDOT platform for ultrasensitive detection of LPS. Electroanalysis 25(2):380–386. https://doi.org/10.1002/elan.201200453
13. Bai L, Chai Y, Pu X, Yuan R (2014) A signal-on electrochemical aptasensor for ultrasensitive detection of endotoxin using three-way DNA junction-aided enzymatic recycling and graphene nanohybrid for amplification. Nanoscale 6(5):2902–2908. https://doi.org/10.1039/c3nr05930h
14. Giovanni M, Setyawati MI, Tay CY, Qian H, Kuan WS, Leong DT (2015) Electrochemical quantification of Escherichia coli with DNA nanostructure. Adv Funct Mater 25(25):3840–3846. https://doi.org/10.1002/adfm.201500940
15. Xie S, Dong Y, Yuan Y, Chai Y, Yuan R (2016) Ultrasensitive lipopolysaccharides detection based on doxorubicin conjugated N-(Aminobutyl)-N-(ethylisoluminol) as Electrochemiluminescence Indicator and self-assembled tetrahedron DNA dendrimers as Nanocarriers. Anal Chem 88(10):5218–5224. https://doi.org/10.1021/acs.analchem.6b00276
16. Chinnappan R, AlAmer S, Eissa S, Rahamn AA, Abu Salah KM, Zourob M (2017) Fluorometric graphene oxide-based detection of salmonella enteritis using a truncated DNA aptamer. Microchim Acta 185(1). https://doi.org/10.1007/s00604-017-2601-9
17. Li P, Yu Q, Zhou L, Dong D, Wei S, Ya H, Chen B, Qin Q (2018) Probing and characterizing the high specific sequences of ssDNA aptamer against SGIV-infected cells. Virus Res 246:46–54. https://doi.org/10.1016/j.virusres.2018.01.006
18. Vu CQ, Rotkrua P, Tantirungrotechai Y, Soontornworajit B (2017) Oligonucleotide hybridization combined with competitive antibody binding for the truncation of a high-affinity aptamer. ACS Comb Sci 19(10):609–617. https://doi.org/10.1021/acscombsci.6b00163
19. Zhou J, Battig MR, Wang Y (2010) Aptamer-based molecular recognition for biosensor development. Anal Bioanal Chem 398(6):2471–2480. https://doi.org/10.1007/s00216-010-3987-y
20. Macdonald J, Houghton P, Xiang D, Duan W, Shigdar S (2016) Truncation and mutation of a transferrin receptor aptamer enhances binding affinity. Nucleic Acid Ther 26(6):348–354. https://doi.org/10.1089/nat.2015.0585
21. Han X, Zhang Y, Nie J, Zhao S, Tian Y, Zhou N (2017) Gold nanoparticle based photometric determination of tobramycin by using new specific DNA aptamers. Microchim Acta 185(1):4. https://doi.org/10.1007/s00604-017-2568-6
22. Almusharraf AY, Eissa S, Zourob M (2018) Truncated aptamers for total and glycated hemoglobin, and their integration into a graphene oxide-based fluorometric method for high-throughput screening for diabetes. Microchim Acta 185(5):256. https://doi.org/10.1007/s00604-018-2789-3
23. Perrier S, Guieu V, Chovelon B, Ravelet C, Peyrin E (2018) Panoply of fluorescence polarization/anisotropy signaling mechanisms for functional nucleic acid-based sensing platforms. Anal Chem 90(7):4236–4248. https://doi.org/10.1021/acs.analchem.7b04593
24. Chen Z, Li H, Jia W, Liu X, Li Z, Wen F, Zheng N, Jiang J, Xu D (2017) Bivalent Aptasensor based on silver-enhanced fluorescence polarization for rapid detection of Lactoferrin in Milk. Anal Chem 89(11):5900–5908. https://doi.org/10.1021/acs.analchem.7b00261
25. Cui L, Zou Y, Lin N, Zhu Z, Jenkins G, Yang CJ (2012) Mass amplifying probe for sensitive fluorescence anisotropy detection of small molecules in complex biological samples. Anal Chem 84(13):5535–5541. https://doi.org/10.1021/ac300182w
26. Liu J, Wang C, Jiang Y, Hu Y, Li J, Yang S, Li Y, Yang R, Tan W, Huang CZ (2013) Graphene signal amplification for sensitive and real-time fluorescence anisotropy detection of small molecules. Anal Chem 85(3):1424–1430. https://doi.org/10.1021/ac3023982
27. Jiang Y, Tian J, Hu K, Zhao Y, Zhao S (2014) Sensitive aptamer-based fluorescence polarization assay for mercury(II) ions and cysteine using silver nanoparticles as a signal amplifier. Microchim Acta 181(11–12):1423–1430. https://doi.org/10.1007/s00604-014-1296-4
28. Li X, Ding X, Li Y, Wang L, Fan J (2016) A TiS2 nanosheet enhanced fluorescence polarization biosensor for ultra-sensitive detection of biomolecules. Nanoscale 8(18):9852–9860. https://doi.org/10.1039/c6nr00946h
29. Shawn E, Lupold BJH, Lin Y et al (2002) Identification and characterization of nuclease-stabilized RNA molecules that bind human prostate Cancer cells via the prostate-specific membrane antigen. Cancer Res 62:4029–4033
30. PWCG A (2009) The shorter the better: reducing fixed primer regions of oligonucleotide libraries for aptamer selection. Molecules 14(4):1353–1369. https://doi.org/10.3390/molecules14041353
31. Kwon YS, Ahmad Raston NH, Gu MB (2014) An ultra-sensitive colorimetric detection of tetracyclines using the shortest aptamer with highly enhanced affinity. Chem Commun (Camb) 50(1):40–42. https://doi.org/10.1039/c3cc47108j
32. Lee EH, Lim HJ, Lee SD, Son A (2017) Highly sensitive detection of bisphenol a by NanoAptamer assay with truncated aptamer. ACS Appl Mater Interfaces 9(17):14889–14898. https://doi.org/10.1021/acsami.7b02377
33. Rockey WM, Hernandez FJ, Huang SY, Cao S, Howell CA, Thomas GS, Liu XY, Lapteva N, Spencer DM, McNamara JO, Zou X, Chen SJ, Giangrande PH (2011) Rational truncation of an RNA aptamer to prostate-specific membrane antigen using computational structural modeling. Nucleic Acid Ther 21(5):299–314. https://doi.org/10.1089/nat.2011.0313
34. Ye H, Duan N, Wu S, Tan G, Gu H, Li J, Wang H, Wang Z (2017) Orientation selection of broad-spectrum aptamers against lipopolysaccharides based on capture-SELEX by using magnetic nanoparticles. Microchim Acta 184(11):4235–4242. https://doi.org/10.1007/s00604-017-2453-3
35. Zhang D, Shen H, Li G, Zhao B, Yu A, Zhao Q, Wang H (2012) Specific and sensitive fluorescence anisotropy sensing of guanine-quadruplex structures via a photoinduced electron transfer mechanism. Anal Chem 84(18):8088–8094. https://doi.org/10.1021/ac302320x